Analysis of Combustion Cycle-to-Cycle Variation in an Optical Single Cylinder Dual-Fuel Engine

Lauterkorn AM, Wang X and Zhao H

)

Abstract

This study aims to improve the dual fuel combustion for low/zero carbon fuels. Seven cases were tested in a single cylinder optical engine and their ignition and combustion characteristics are compared. The baseline case is the conventional diesel combustion. Four cases are diesel-gas (compressed natural gas) dual-fuel combustion operations, and two cases are diesel-hythane combustion. The diesel fuel injection process was visualized by a high-speed copper vapour laser. The combustion processes were recorded with a high-speed camera at 10000 Hz with an engine speed of 1200 rpm. The high-speed recordings for each case included 22 engine cycles and were postprocessed to create one spatial overlapped average combustion image. The average combustion cycle images were then further thresholded and these images were then used in a new method to analyze the cycle-to-cycle variation in a dimensionless, for all cases comparable value. Furthermore, the ignition delay and heat release profile of each case are analyzed. The results showed the lowest deviation from the complete overlap for the pure Diesel case and the Hythane Cases since the flames are more concentrated in these. From these studies, it can be concluded that the cyclic variation for the pure diesel combustion is mostly caused by the different swirl speeds in the piston bowl. The diesel-gas dual-fuel combustion with earlier pilot injections have lower cyclic variation due to a wider spread of the combustible mixture. The usage of hythane as main fuel instead of methane results in a about 10% faster combustion and more concentrated flames areas.

Introduction

Significant engine research and development works have been carried out to improve the engine's efficiency and simultaneously reduce their emissions. One of the approaches to achieve this for compression ignition engines is dual-fuel combustion, which allows the low and zero carbon fuels to be used in the existing engines. However, this approach faces difficulties like unstable combustion at low load and violent knocking at very high load conditions. Therefore, studies on optical engines are necessary to better understand and improve the dual-fuel combustion.

In order to tackle the rising demand for higher efficiency engines with simultaneously lower pollutant emissions, the processes within an Internal Combustion Engine (ICE) need to be further investigated to gain better understanding of the impact of key parameters. One way to lower the engine emissions is the usage of emissions and exhaust aftertreatments [1]. One way to improve these engines is by combining Computational Fluid Dynamics (CFD) simulations and experiments on an optical engine in order to visualize the combustion events like ignition delay, combustion duration and flame propagation within the cylinder. In particular, more studies are needed on the ignition and combustion processes of biofuels, low carbon and zero carbon fuels which are essential for the net-zero transport. One of the approaches to use such fuels is dual-fuel combustion, where a main fuel, which could not be compression ignited or only with very high compression ratios, is ignited by a pilot fuel which auto ignites under the given conditions and therefore initiates the combustion of the main fuel.

The main advantage of dual-fuel engines is that they can be achieved on the current Compression Ignition (CI) engines by adding a Port Fuel Injector (PFI). However, the dual-fuel combustion engine operation tends to experience unstable combustion at low load and violent knocking combustion at very high load conditions. Because of this, the maximum substitution rate can often not be reached [2, 3]. A typical dual-fuel mixture is Diesel-Natural Gas (NG), because the main component of NG is Methane, which has a much lower carbon content than diesel. However, the Global Warming Potential (GWP) of unburnt CH_4 is 25 times the GWP of CO_2 [4] and therefore it is critical to ensure the complete combustion of methane in order to reduce the Green-House Gas emissions. In-cylinder optical measurements are well suited to gain the insight into the ignition and combustion processes of the dual-fuel engine operation. Various methods have already been used to investigate the in-cylinder mixing and combustion processes, such as Mie-scattering, Laser Induced Fluorescence (LIF), Schlieren and Shadowgraphy [5, 6, 7, 8].

Dronniou et al. [9] used Mie-scattering to observe the combustion processes, demonstrating the effects of different equivalence ratios of the fuel. Furthermore, Kim, Park, and Bae [10] showed the usage of flame visualization to observe the combustion phenomena with focus on the flame propagation, investigating the effect of different injection timings. Zhao et al. [11] focused on the dual-fuel mixture formation observation to investigate the distribution of the main fuel in the combustion chamber with LIF using NO_2 as a tracer. For the observation of the Diesel Spray, Schlieren and Shadowgraphy can be

employed, as has been shown by Lazzaro [12]. Many other Studies focus on testing and comparing different fuels to improve dual-fuel combustion [13, 14, 15].

However, many of these optical studies focus on the flame propagation or analysis of the mixture formation. In addition to these observations, dual-fuel recordings can be used to construct average combustion cycles and analyze the cycle-cycle variation with these. This would produce valuable results to validate and advance CFD studies [16, 17, 18] which focus on this topic. Mertz and Verhelst [19] have summarized different simulation approaches for dual fuel engines. This study focuses on investigating the dual-fuel combustion with direct-injection diesel as the pilot ignition fuel and port fuel injected Natural Gas and Hythane as the main fuel, with the object of using the combustion images to analyze the cycle-to-cycle variation.

The motivation for this study is to improve the dual fuel combustion because of their potentially lower emissions when using NG/Hythane. Since these tend to be unstable in low load conditions, it is necessary to further study the combustions and explicitly the cycle-to-cycle variation. Previous studies on the cycle-to-cycle variation have been carried out by Cheng et al [20], however, the analysis focused on the spatial distribution of the flames and not on the overall flame area and different fuels. A different approach was carried out by Pasunurthi et al. [21], who simulated the cycle-to-cycle variation and compared them to an experimental engine. In this study, a new method will be used by creating overlapping averages for each case and the referring the individual cases to it, in order to have a dimensionless value that makes all cases comparable to each other. Two test cases with Hythane are carried out since it has a faster combustion speed due to the Hydrogen, to analyze which of the fuels has a more stable and efficient dual fuel combustion.

Methodology

The experiments to study the dual-fuel combustion were carried out in an optical single cylinder engine. The engine is built with a Bowditch extended piston design with an optical window in the piston top of 56 mm diameter and also has three small windows for the side view access of the chamber. For this study only the bottom access to the combustion chamber via the piston window was used. The external illumination of the combustion chamber was provided by a copper vapour Laser in a similar setup to [22]. The Laser repetition rate was 10000 Hz with a pulse duration of 10-40 ns and a wavelength of 512 nm. The short pulse duration of the laser leads to a very short illumination time which results in less motion blur and therefore sharper images. The images were recorded with a PHOTRON Fastcam Mini AX 100 with a matching framerate of 10000 Hz and a shutter speed of 950000 1/s respectively with a shutter opening duration of approximately 1.05 μs per frame. The image resolution was set to 512 x 512 pixels to record square images through the window in the piston top. The lens used to capture the images was a Nikon UV Nikkor 105mm f/4.5s. The details of the engine and optical set up are summarized in Table 1.

Table 1: Properties of the optical equipment

Equipment	Parameters	Values
Ricardo Optical Single Cylinder Engine	Bore	86 mm
	Stroke	86 mm
	Swept Volume	499 cm^3
	Compression Ratio	16:1
	Piston Window Diameter	56 mm
Oxford Lasers Copper Vapour Laser	Wavelength	512 nm
	Pulse duration	10-40 ns
	Repetition rate	10000 Hz
Photron Fastcam Mini AX 100	Framerate	10000 Hz
	Shutter speed	950000 1/s
	Resolution	512 x 512 Pixel
Nikon UV Nikkor Lens	Focal length	105 mm
	Aperture	f 4.5

The schematics of the optical measurement are shown in Figure 1. The Laser is connected to a beam expander at the end of an optical fiber to illuminate the combustion chamber through the 45° angled mirror below the window in the extended piston top. The Laser radiation is then reflected in the combustion chamber, back to the mirror and from there it is recorded by the camera.
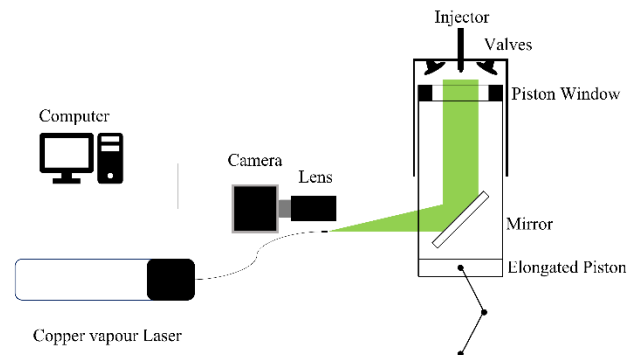

Figure 1: Schematics of the optical tests

Simultaneous to the optical recordings, the pressure data was recorded with a Kistler In-Cylinder pressure sensor and National Instruments cRIO 9066 Data acquisition system using a code written in LabView. Seven Cases with different injection timings and durations were combined to observe the ignition sites and flame

propagation area within the combustion chamber. For all the experiments in this study the engine speed was kept constant at 1200 rpm, the injection pressure for the Diesel was 500 bar and for the NG/Hythane it was kept to 5 bar. The Diesel was direct injected and the NG/Hythane was port fuel injected. The natural gas composition is shown in Table 2, with the minima and maxima of the volumetric percentage that each component can have in the mixture, according to the manufacturer.

Table 2: Natural Gas composition

Component	Volumetric percentage (min & max)
Methane	80 - 90
Ethane	< 12
Propane	< 4
Butane	< 0.5
Isobutane	< 0.5
Isopentane	< 0.5
Nitrogen	< 15
Carbon Dioxide	< 5

From the seven cases chosen for this study, one represents the pure diesel combustion, and the others represent dual-fuel combustion with varying injection strategies and durations. The used Hythane mixture consist of 20% Hydrogen and 80% Methane.

Prior to the current studies, a number of engine experiments were performed, during which the diesel injection timings were adjusted, to optimize the Indicated Mean Effective Pressure (IMEP) for each individual case. The first case A1 represents the pure diesel combustion with a split injection and is used as the baseline case. The diesel was injected twice at 14◦ and 5◦ Crank Angle (CA) before Top-Dead-Centre (TDC) with a 50:50 Pulse duration split of 0.45 ms duration per injection. Case B1 and B2 represent the dual-fuel combustion with 50:50 split pilot diesel fuel injections before TDC and a single NG main fuel injection in the intake port. Case C1 has a 50:50 split pilot diesel fuel injection, where the second one is after TDC and a single NG main fuel injection. Case C2 has a non-uniformly split pilot diesel fuel injection with the second one after TDC and 50:50 split double NG injections. Cases D1 and D2 both have a non-uniformly split pilot diesel fuel injection with the second one occurring after TDC. The main fuel injection for D1 was a single hythane injection and for the Case D2 it was 50:50 split double hythane injections. A summary of the injection durations, fuel masses approximations and IMEP for each case is shown in Table 3 and the injection timings for all cases are shown in Table 4. The Diesel was split injected in all cases, therefore, the Diesel injection timing and duration shows two values. Due to the nature of the engine control system, the injection duration is limited to maximum 5 ms and longer injections for the NG/Hythane had to be split up into multiple ones.

Since those are closed valve injections, it is believed, that this has no altering effect compared to a continuous injection.

Table 3: Test cases injection duration and Mass

Case	Diesel injec. durat. [ms]	Diesel Mass appro. [mg]	Main fuel injec. durat. [ms]	NG Mass appro. [mg]	Hythane Mass appro. [mg]	IMEP [bar]
A1	0.45 + 0.45	2 x2.87	None	None	None	2.18
B1	0.4 + 0.4	2 x1.83	2.0	1.77	None	0.51
B2	0.4 + 0.4	2 x1.83	2.0	1.77	None	2.11
C1	0.33 + 0.33	2 x0.37	2.0	1.77	None	1.84
C2	0.3 + 0.33	0.3+0.37	4 .0+ 4.0	2 x 3.02	None	6.53
D1	0.3 + 0.33	0.3+0.37	2.0	None	1.77	3.72
D2	0.3 + 0.33	0.3+0.37	4.0 + 4.0	None	2 x 3.02	7.88

Table 4: Test cases injection timing

Case	Diesel injec. timing [◦CA before TDC]	NG injec. timing [◦CA before TDC]	Hythane injec. timing [◦CA before TDC]
A1	14 + 5	None	None
B1	15 + 5	300	None
B2	10 + 5	300	None
C1	15 + (-2)	300	None
C2	15 + (-1)	360 + 320	None
D1	15 + (-1)	None	300
D2	12 + (-1)	None	360 + 320

Results and Discussion

The recorded combustion images were post-processed using a code written in Python 3.8. The code is used to firstly identify the region

of the piston window as shown by image (a) to image (b) in Figure 2. The images are then masked and cropped as shown by image (b) to image (c) in Figure 2. These steps exclude all the unnecessary information and unwanted laser reflections in the recordings. Afterwards, the cropped and masked images are binarized with a threshold, with a minimum pixel value of 75, set to show only the flame contours as shown in image (c) to image (d) in Figure 2. This change was implemented since this study aims to analyze the flame area and not the intensity of individual regions.
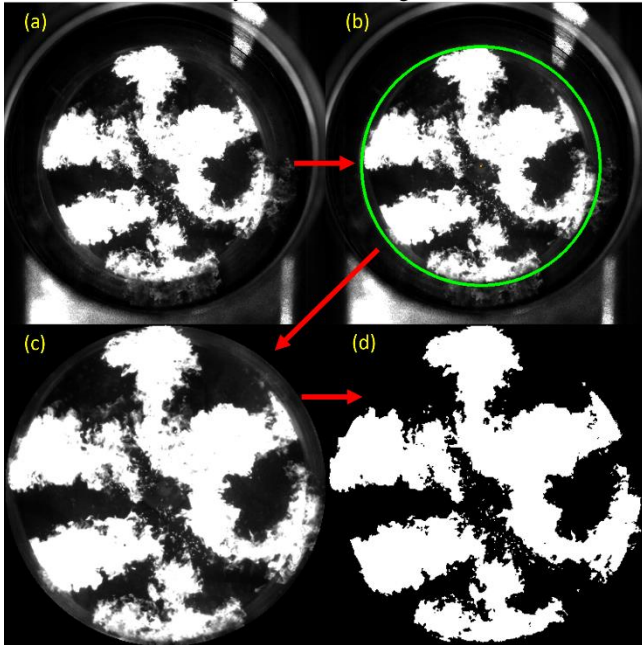
Figure 2: Image Processing via Masking and Binarization

Similar to the approach to the combustion images reported in [23], after these processing steps, the binarized images are filtered with an area closing function to fill the holes within the flames below a threshold area of 25 pixels to make the image uniformly as shown by image (e) to image (f) in Figure 3. Furthermore, the area opening function is applied to eliminate small islands below a threshold area of 10 pixels as depicted in Figure 3 (f) to image (g). Afterwards a gaussian filter is applied to smooth the contours of the flame, where the sigma of the filter was chosen to be 0.2. The effects of the filter would be minor to not falsify the original outlines as shown in image(g) to (h) in Figure 3.
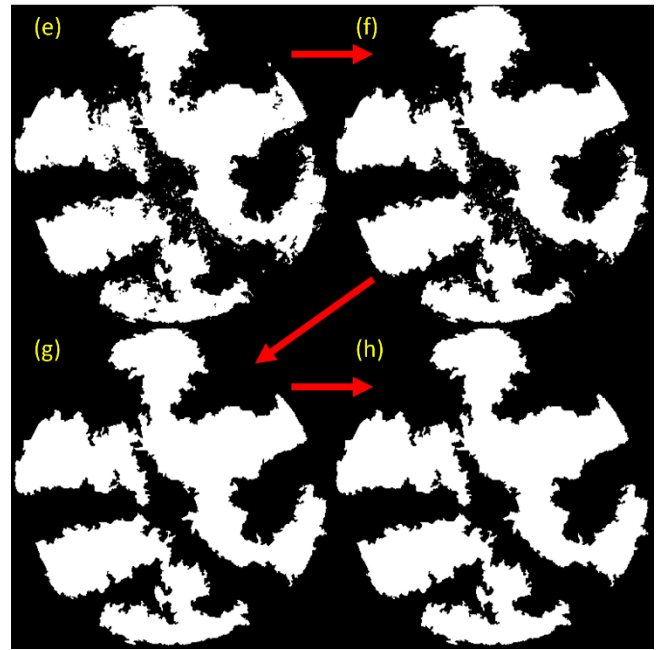

Figure 3: Image processing via Scikit-Image and Scipy

In this study, multiple engine cycles were recorded in order to build images for the average flame structure and study the cycle-to-cycle variations. The maximum number of recordings per test case for the Mini AX 100 at 512 x 512 pixels are limited to 21829 images, which corresponds to about 22 engine combustion cycles at 1200 rpm. The code execution starts with the first image frame of the pilot diesel injection and saves the following 100 frames to a separate folder for each cycle. The average combustion image at each crank angle is constructed as schematically shown in Figure 4. The highest concentration of visible combustion sites is shown in red (100 % overlap of the pixels with combustion) and non-visible combustion sites are shown in blue.
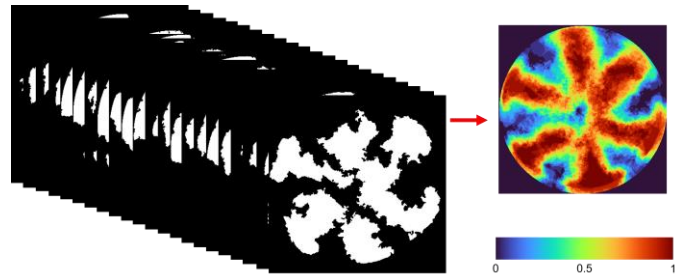

Figure 4: The average flame image produced by stacking combustion images from 22 cycles at the same crank angle

The last step is to analyze the flame area pixel distribution and its change during the combustion process. This was realized by counting the number of the non-zero pixels of the overlap areas and dividing them by the total number of pixels in the average image, to create the curve called "overlap". Since the average images were created by stacking 22 images which can either have a pixel value of 255 (flame present) or 0 (no flame observed), the maximum value of the overlap pixels is also 255. As a result, any pixel in the average image can only take a fixed value, for example a pixel where 13 cycles overlap would take the value:

$$Pixel_{value} = \frac{13}{22} \times 255 \approx 150.68$$

In order to analyze the cycle-to-cycle variation in the combustion sites and identify the location of most combustion taking place, the level of overlap was then applied to the average images. Firstly, when the threshold is set to 35 for pixels of the averaged images, pixels with combustion in 3 or more cycles will be included. As the threshold is increased to 82, pixels with combustion in 7 or more cycles are shown. In turn, the minimum number of cycles with overlap combustion pixels will increase to 11, 15 and 18, as the threshold is raised to 128, 175 and 210. The schematics of this step are illustrated in Figure 5.
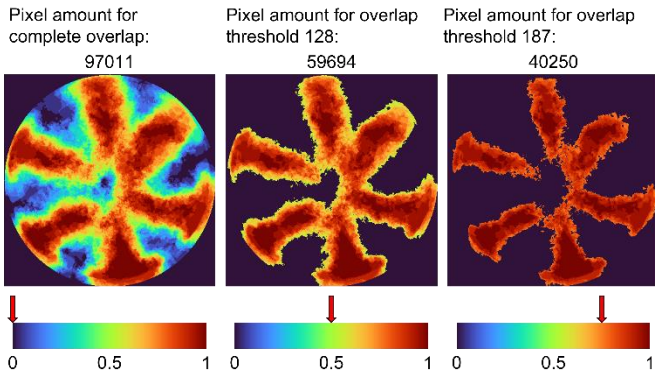
Figure 5: Complete and threshold images

In the last step, the deviation of threshold images at a given crank angle from the complete overlap images was determined by dividing the number of images of a given threshold (for example 150 so that minimum 13 cycles have to overlap) to the amount of the complete overlap pictures (no threshold, all overlapping pixels are counted) and then subtracting it from 1, as shown in the following equation:

$$Deviation = 1 - \frac{Pixelcount_{thresholded}}{Pixelcount_{complete\ overlap}}$$

This was done to show the cycle-to-cycle variation in more comprehensible way, since non variant cycles would be overlapping as much as possible and nearly never reach the maximum deviation of 1. For cases with stronger combustion the pixel analysis is deteriorated since the residues pollute the piston window and limit the camera view. Therefore, the deviation of the threshold curves to the complete overlap serves as comprehensive comparison.

Based on the above analysis, the results for the seven cases are shown in Figure 6 to Figure 12. In each Figure, the upper graph shows the complete overlap pixels curve ("overlap") together with the in-cylinder pressure ("Cylinder pressure") and the thresholded overlap curves for 3, 7, 11, 15 and 18 cycles overlapping (indicated by their thresholds in the curve descriptions) and the lower one showing the deviation curves for the different thresholds with similar description. To aid the analysis, the graphs also include markers for the injection timings, the start of the combustion as well as the Crank Angles where 50% and 90% of mass fractions were burnt (CA50 and CA90).
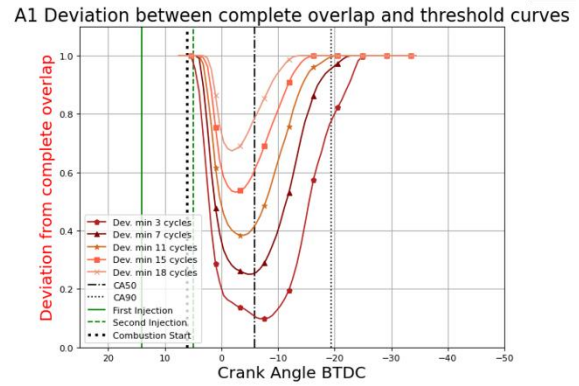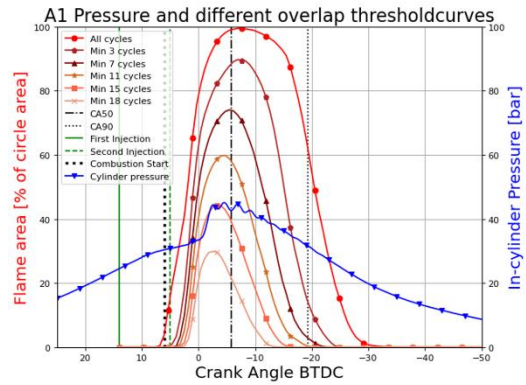

Figure 6: Case A1 average image analysis, pixel count for different thresholds and pressure curve (upper graph), deviation for different thresholds (lower graph)
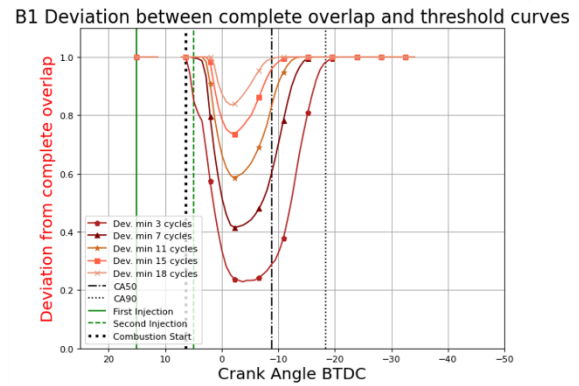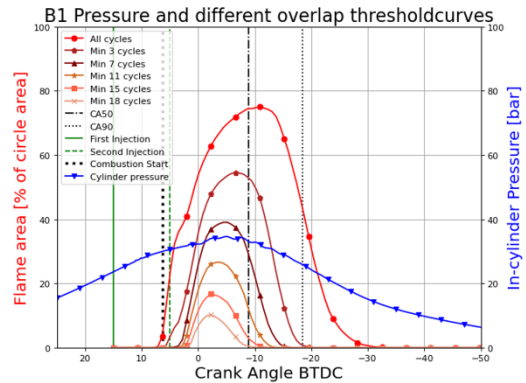

Figure 7: Case B1 average image analysis, pixel count for different thresholds and pressure curve (upper graph), deviation for different thresholds (lower graph)
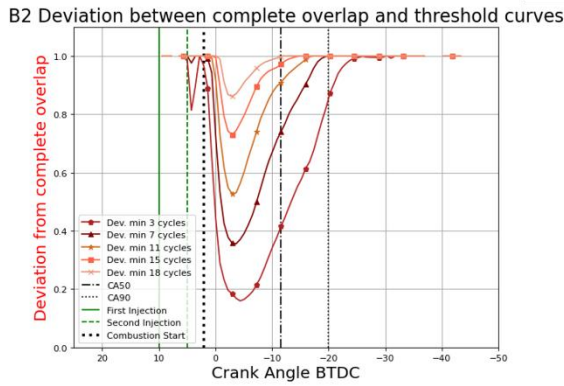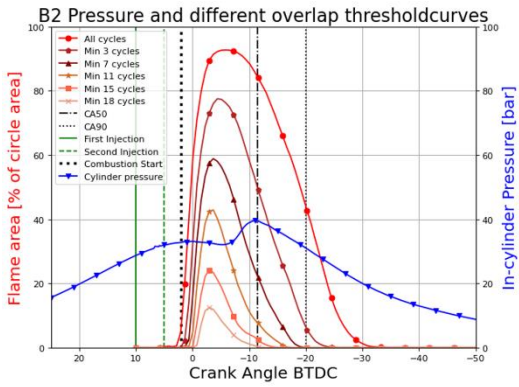
Figure 8: Case B2 average image analysis, pixel count for different thresholds and pressure curve (upper graph), deviation for different thresholds (lower graph)
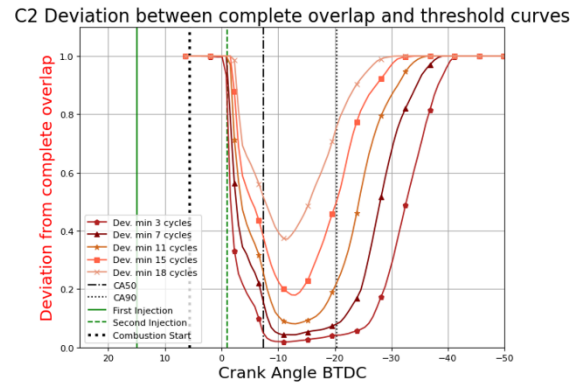

Figure 10: Case C2 average image analysis, pixel count for different thresholds and pressure curve (upper graph), deviation for different thresholds (lower graph)
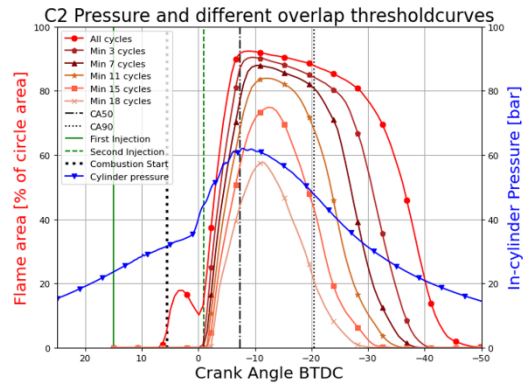

Figure 9: Case C1 average image analysis, pixel count for different thresholds and pressure curve (upper graph), deviation for different thresholds (lower graph)

Figure 11: Case D1 average image analysis, pixel count for different thresholds and pressure curve (upper graph), deviation for different thresholds (lower graph)

10/22/2022

Figure 12: Case D2 average image analysis, pixel count for different thresholds and pressure curve (upper graph), deviation for different thresholds (lower graph)
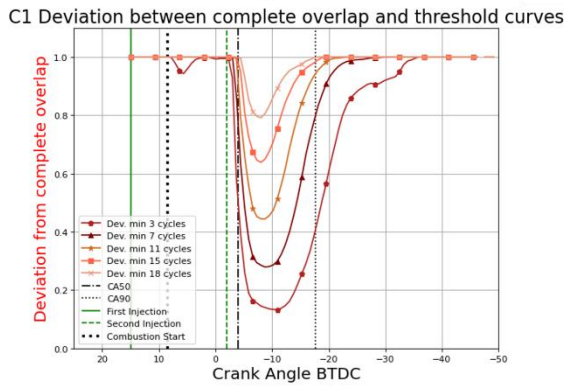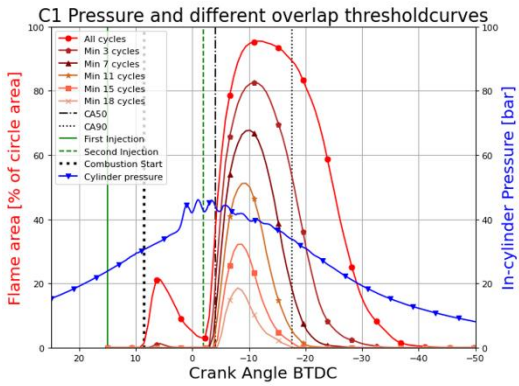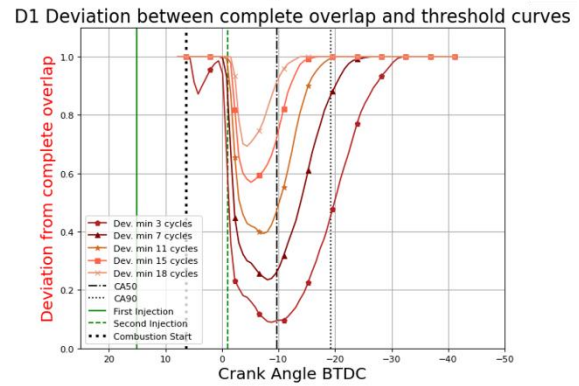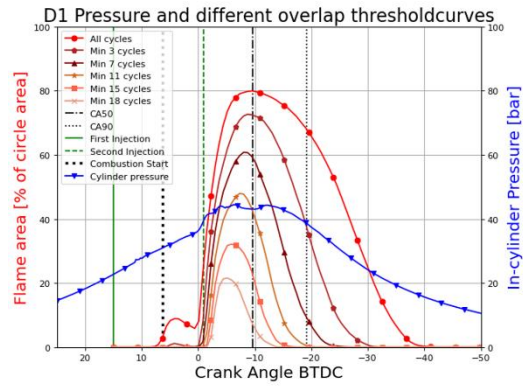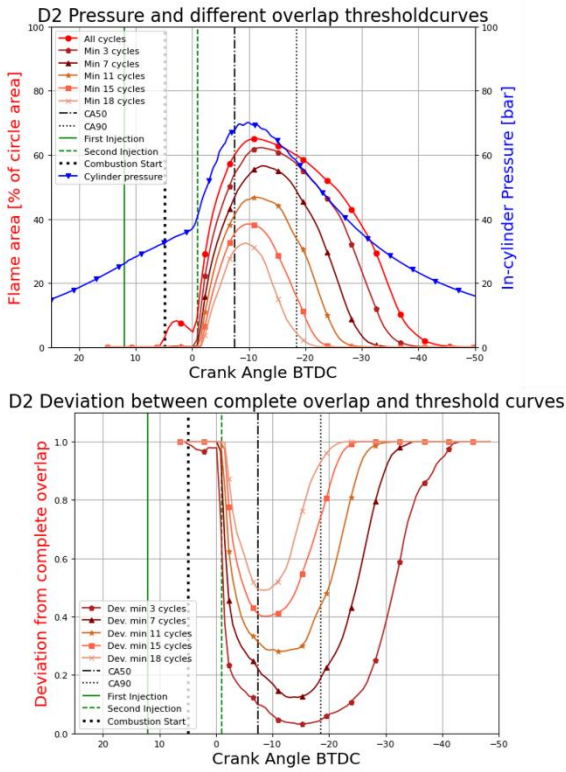
The flame image analysis results show that the deviation or cycle-to-cycle variation for the case A1 is low with an overall uniform distribution of combustion sites. For the case B1 the combustion sites are less uniform in the beginning of the combustion between 5 CA BTDC and TDC. The graphs for case B2 show low deviation with an overall low in-cylinder pressure. Cases C1 and C2 have a high deviation in the beginning of the combustion and become more stable after the second injection at -2 CA BTDC for C1 and -1 CA BTDC for C2. Case D1 and D2 behave similar to Case C1 and C2, but the combustion happens more rapidly, due to the presence of the Hydrogen. It can also be observed that the CA 50 is close to the peak of the pixel curves except for Case C1 where it was reached nearly 10 CA earlier, indicating that the combustion itself was weak and not all of the fuel reacted. Furthermore, the combustion cases C2 and D2, where the influences of the gas were dominant, show a longer duration until no pixels are observed anymore, which is due to the longer combustion duration of the Natural Gas compared to Diesel or Hydrogen. Also, Cases C1, C2, D1 and D2 show a high deviation in the beginning of the combustion as well as in the end, which is due to the influences of the natural gas which shows more cycle-to-cycle variation then the Diesel. These influences are vanishing in the thresholding curves since not many cycles overlap in the irregular combustion sites. For an overview of the flame development during the combustion, the averaged images for each case at 5 CA and 10 CA ATDC are shown in Figure 13.
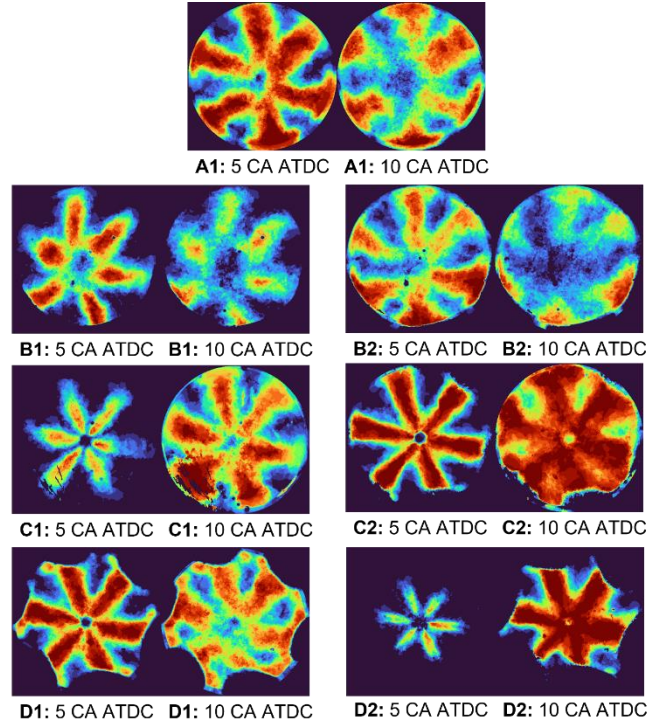

Figure 13: Averaged combustion images for 5 and 10 CA ATDC for each test case

Afterwards, the ignition and heat release processes are analyzed in terms of the ignition delays, which were determined from the first injection to the start of the combustion, the CA50 and the CA90. The ignition delay was calculated by the time elapsed between the start of the first Diesel injection and the first image win which flames were recorded for each case. The results are summarized in Table 5. It can be observed in Figure 13 that the Case A1 which reaches the CA50 close to 5 CA ATDC shows a very concentrated flame area in the pattern of the diesel spray, whereas Case B2 which reaches the CA50 later, only shows small, concentrated flame areas in a similar pattern.

Table 5: Ignition delays, CA50 and CA90

Case	Ignition delay	CA50 ATDC	CA90 ATDC
A1	7.92	5.79	19.32
B1	9.36	8.91	18.44
B2	7.92	11.49	19.96
C1	7.92	4.06	17.67
C2	9.36	7.36	20.42
D1	8.64	7.46	19.24
D2	7.08	9.67	18.46

10/22/2022

It can be observed that the ignition delay for case D2 is the shortest due to the presence of the Hydrogen. For Case A1, B2 and C1 the Ignition delay is nearly the same value because of the dominant influence of the diesel. For the Cases B1, C2 and D1 the dominant influence of the gas delays the ignition further compared to the other cases.

Furthermore, the Heat Release Rate (HRR) and Net Heat Release (NHR) for each case were calculated and are shown in Figure 14 to Figure 16. The formula used for calculating the HRR was the following:

$$HRR = \frac{\gamma}{\gamma - 1} p \frac{dV}{dt} + \frac{1}{\gamma - 1} V \frac{dp}{dt}$$

The value for gamma is normally not a fixed one but for these calculations it was set to 1.3 since this is a typical value for Diesel engines and the in-cylinder temperature data was not available. Furthermore, the crevice flows were neglected. This calculation does not 100% display the real HRR for the dual fuel cases, especially when Hythane was used, but the calculations give a simplified indication to make the cases comparable. Due to vibrations in the pressure signal that could not been completely smoothed out, some positive HRR can be observed before the15 CA. The HRR of Case A1 is typical for pure diesel combustion with a peak release rate shortly after TDC from the premixed combustion phase and a second small peak after CA50 from the mixing-controlled combustion phase [24]. The HRR for Case B1 also shows two distinguishable peaks for the premixed and mixing-controlled combustion, although they are nearly at the same height since the overall NHR is lower than in the pure Diesel Case. Case B2 shows a dominant premixed combustion again while Case C1 has an overall high peak HRR with a significant mixing-controlled combustion. For the Case C2 the premixed combustion has the highest peak of all cases, resulting in the highest NHR in Diesel-NG combustion. The Cases D1 and D2 show similar Heat releases to the Methane cases, but with the overall highest IMEP of all cases for D2 since the Hythane combustion happens more rapidly.
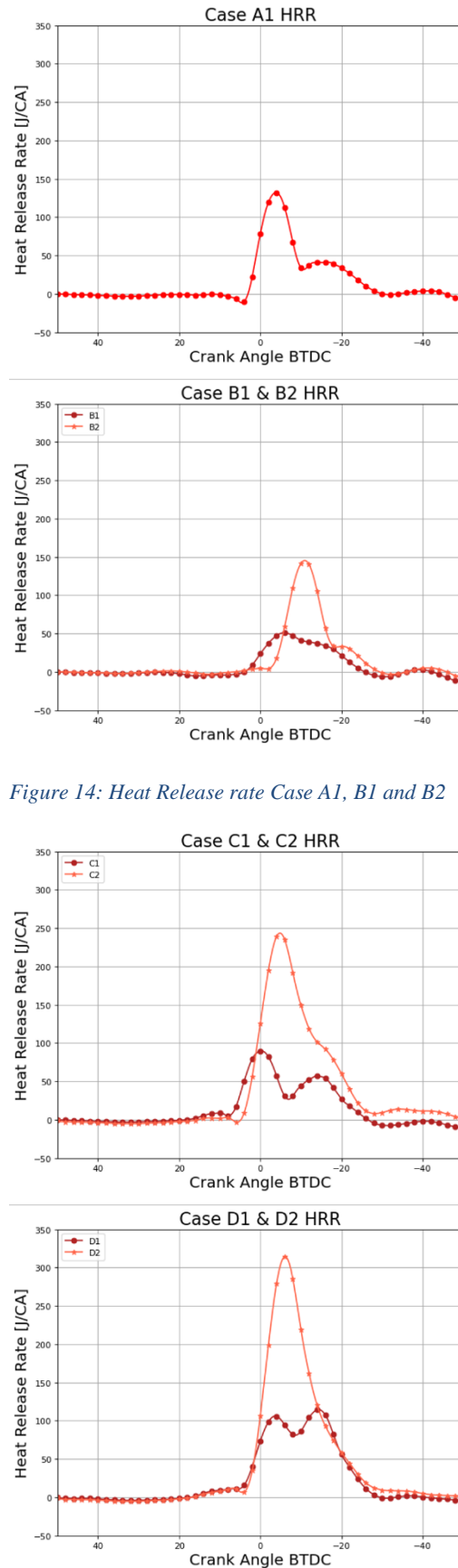

Figure 14: Heat Release rate Case A1, B1 and B2

Figure 15: Heat Release rate Case C1, C2, D1 and D2
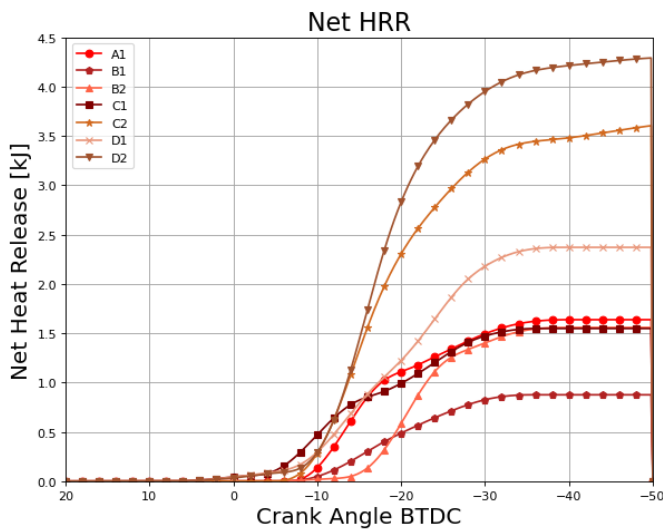
10/22/2022

Figure 16: Net Heat Release

As mentioned initially, the injection timings were adjusted to optimize the IMEP of each case. Since the combustion Images in this analysis have been binarized, there is no direct comparison made between the flame intensity and the efficiency. However, the dual-fuel cases with the lowest deviation show the highest heat release, indicating a relation between lower cycle-to-cycle variation and combustion efficiency.

Conclusion

In this study, combustion recordings taken at a single cylinder optical engine have been processed and compared. Furthermore, the in-cylinder pressure curves have been analyzed and the heat releases calculated. A new method was proposed to analyze the cycle-to-cycle variation by creating an overlap cycle for each test case and then comparing thresholded curves to it. By this, a deviation curve was created, which made all cases comparable, independent on how the flames develop or how much they dirty the piston glass during the observation. The results from the image and heat release analyses of the test cases can be summarized as follows:

- The cyclic variation for the pure diesel combustion is overall low and is mostly caused by cyclic varying swirl motion velocities in the piston bowl.

- The dual-fuel test cases with earlier split pilot injections BTDC have lower cyclic variation due to more uniform distribution of combustible mixture in the cylinder and the dominant influence of the diesel injection and combustion.

- The dual-fuel test cases with pilot injections BTDC and ATDC have high cyclic variations between the first and second diesel injection since the start of the low reactivity dual-fuel combustion occurs randomly in the combustion chamber. After the second injection the cyclic variation is

reduced as more ignition sites are formed from the second injection.

- The increase of the NG amount in the Case C2 leads to higher cycle variation after the second diesel injection when more dominant NG combustion effects occur.

- The dual fuel combustions are less reactive than the pure diesel ones if the injection timing for the diesel are similar to the pure diesel case.

- Changing the dual fuel injection timings to delay the second diesel injection to occur after the combustion start leads to an ignition of the diesel spray as soon as it is injected and increases the heat release drastically.

Abbreviations

CA Crank Angle.

CFD Computational Fluid Dynamics.

CI Compression Ignition.

DI Direct Injector.

GWP Global Warming Potential.

HRR Heat Release Rate.

ICE Internal Combustion Engine.

IMEP Indicated Mean Effective Pressure.

LIF Laser Induced Fluorescence.

NG Natural Gas.

NHR Net Heat Release

PFI Port Fuel Injector.

TDC Top-Dead-Centre.

References

1. Reşitoğlu, İ.A., Altinişik, K. & Keskin, A. The pollutant emissions from diesel-engine vehicles and exhaust aftertreatment systems. Clean Techn Environ Policy 17, 15–27 (2015). https://doi.org/10.1007/s10098-014-0793-9
2. Karim, G.A. (2015). Dual-Fuel Diesel Engines (1st ed.). CRC Press. https://doi.org/10.1201/b18163 ISBN 9780429069765
3. Papagiannakis, R., Hountalas, D., Rakopoulos, C., and Rakopoulos, D., "Combustion and Performance Characteristics of

10/22/2022

a DI Diesel Engine Operating from Low to High Natural Gas Supplement Ratios at Various Operating Conditions," SAE Technical Paper 2008-01-1392, 2008, https://doi.org/10.4271/2008-01-1392

4. Muralidharan, M., Srivastava, A., and Subramanian, M., "A Technical Review on Performance and Emissions of Compressed Natural Gas - Diesel Dual Fuel Engine," SAE Technical Paper 2019-28-2390, 2019, https://doi.org/10.4271/2019-28-2390.

5. Zhao, Hua. "Laser Diagnostics and Optical Measurement Techniques in Internal Combustion Engines." (2012). https://doi.org/10.4271/r-406 ISBN 978-0-7680-7766-7

6. Gleis, S., Frankl, S., Waligorski, D., Prager, D. et al., "Investigation of the High-Pressure-Dual-Fuel (HPDF) combustion process of natural gas on a fully optically accessible research engine," SAE Technical Paper 2019-01-2172, 2019, https://doi.org/10.4271/2019-01-2172.

7. Rochussen J, McTaggart-Cowan G, Kirchen P. Parametric study of pilot-ignited direct-injection natural gas combustion in an optically accessible heavy-duty engine. International Journal of Engine Research. 2020;21(3):497-513. doi:10.1177/1468087419836877.

8. Srna, A., Bruneaux, G., Von Rotz, B., Bombach, R. et al., "Optical Investigation of Sooting Propensity of n-Dodecane Pilot/LeanPremixed Methane DualFuel Combustion in a Rapid Compression-Expansion Machine," SAE Int. J. Engines 11(6):1049-1068, 2018, doi:10.4271/2018-01-0258.

9. Dronniou, N., Kashdan, J., Lecointe, B., Sauve, K. et al., "Optical Investigation of Dual-fuel CNG/Diesel Combustion Strategies to Reduce CO2 Emissions," SAE Int. J. Engines 7(2):873-887, 2014, https://doi.org/10.4271/2014-01-1313.

10. Kim, W., Park, C., and Bae, C., "Combustion Phenomena and Emissions in a Dual-Fuel Optical Engine Fueled with Diesel and Natural Gas," SAE Int. J. Adv. & Curr. Prac. in Mobility 4(2):502-513, 2022, https://doi.org/10.4271/2021-01-1175.

11. Zhao, F., Taketomi, M., Nishida, K., and Hiroyasu, H., "PLIF Measurements of the Cyclic Variation of Mixture Concentration in a SI Engine," SAE Technical Paper 940988, 1994, https://doi.org/10.4271/940988.

12. Lazzaro, M., "High-Speed Imaging of a Vaporizing GDI Spray: A Comparison between Schlieren, Shadowgraph, DBI and Scattering," SAE Technical Paper 2020-01-0326, 2020, https://doi.org/10.4271/2020-01-0326.

13. B.B. Sahoo, N. Sahoo, U.K. Saha, Effect of engine parameters and type of gaseous fuel on the performance of dual-fuel gas diesel engines—A critical review, Renewable and Sustainable Energy Reviews, Volume 13, Issues 6–7, 2009, Pages 1151-1184, ISSN 1364-0321, https://doi.org/10.1016/j.rser.2008.08.003.

14. Wagemakers, A. and Leermakers, C., "Review on the Effects of Dual-Fuel Operation, Using Diesel and Gaseous Fuels, on Emissions and Performance," SAE Technical Paper 2012-01-0869, 2012, https://doi.org/10.4271/2012-01-0869.

15. Selim, M. and Saleh, H., "Performance and Noise of Dual Fuel Engine Running on Cottonseed, Soybean Raw Oils and Their Methyl Esters as Pilot Fuels," SAE Technical Paper 2020-01-0811, 2020, https://doi.org/10.4271/2020-01-0811.

16. Jupudi, R., Finney, C., Primus, R., Wijeyakulasuriya, S. et al., "Application of High Performance Computing for Simulating Cycle-to-Cycle Variation in Dual-Fuel Combustion Engines," SAE Technical Paper 2016-01-0798, 2016, https://doi.org/10.4271/2016-01-0798.

17. Fraioli, V., Beatrice, C., Di Blasio, G., Belgiorno, G. et al., "Multidimensional Simulations of Combustion in Methane-Diesel Dual-Fuel Light-Duty Engines," SAE Technical Paper 2017-01-0568, 2017, https://doi.org/10.4271/2017-01-0568.

18. Millo, F., Accurso, F., Piano, A., Fogla, N. et al., "Development and Validation of a Multi-zone Predictive Combustion Model for Large-Bore Dual-Fuel Engines," SAE Int. J. Engines 15(5):703-718, 2022, https://doi.org/10.4271/03-15-05-0038.

19. : Merts, M. and Verhelst, S., "Literature Review on Dual-Fuel Combustion Modelling," SAE Technical Paper 2019-24-0120, 2019, doi:10.4271/2019-24-0120.

20. Qiang Cheng, Zeeshan Ahmad, Ossi Kaario, Larmi Martti, "Cycle-to-cycle variations of dual-fuel combustion in an optically accessible engine", Applied Energy, Volume 254, 2019, 113611, ISSN 0306-2619,https://doi.org/10.1016/j.apenergy.2019.113611.

21. Pasunurthi, S., Jupudi, R., Wijeyakulasuriya, S., Gubba, S. et al., "Cycle to Cycle Variation Study in a Dual Fuel Operated Engine," SAE Technical Paper 2017-01-0772, 2017, doi:10.4271/2017-01-0772.

22. Zambare, V. and Winterbone, D., "A Photographic Investigation of Multi-Stage Fuel Injection in a Single Cylinder DI Diesel Engine," SAE Technical Paper 1999-01-1501, 1999, https://doi.org/10.4271/1999-01-1501.

23. Rochussen J, Kirchen P. Characterization of reaction zone growth in an optically accessible heavy-duty diesel/methane dual-fuel engine. International Journal of Engine Research. 2019;20(5):483-500. doi:10.1177/1468087418756538.

24. GOMES, F. A. F. et. al. A simplified method for the computation of the premixed mode heat release in di diesel engines. In: BRAZILIAN CONGRESS OF THERMAL SCIENCES AND ENGINEERING - ENCIT, 17th., 25 a 28 nov. 2018, Águas de Lindóia - SP – Brazil. Anais[…], Águas de Lindóia - SP – Brazil, 2018.

10/22/2022

Dear Reviewers,

The authors would like to thank the reviewers for their positive and constructive feedback, which helped to improve the paper. Corrections/answers to the questions and comments raised in the latest version to the paper are addressed below:

Reviewer #317831

Question 1: The Abstract should contain answers to the following questions: What problem was studied and why is it important? What methods were used? What are the important results? What conclusions can be drawn from the results? What is the novelty of the work and where does it go beyond previous efforts in the literature? Please include specific and quantitative results in your Abstract, while ensuring that it is suitable for a broad audience. References, figures, tables, equations and abbreviations should be avoided. In this sense, it would be needed that you clarify why natural gas and why an optical engine to study cycle to cycle variation.
Discussion: Thank you for the suggestion, the following information is in the abstract:
- *Which problem and Importance?* -> Unstable dual fuel combustion at low loads needs to be improved in order to support the goal of the net-zero transport
- *Which methods?* -> High speed recordings of the combustion
- *Important results?* -> The diesel-gas dual-fuel combustion with earlier pilot injections have lower cyclic variation due to wider spread of combustible mixture. The usage of hythane as main fuel instead of methane results in a faster combustion and more concentrated flames.
- *Novelty?* -> The cyclic variation of the combustion cycles is observed by creating an overall flame image and then referring each cycle to it in order to create a dimensionless, over all cases comparable value that is thought to help understand the combustion cases

Changes to the manuscript: Specific and quantitative results were added to the abstract

Question 2: . The originality of the paper needs to be stated clearly. It is of importance to have sufficient results to justify the novelty of a high-quality journal paper. The Introduction should make a compelling case for why the study is useful along with a clear statement of its novelty or originality by providing relevant information and providing answers to basic questions such as: What is already known in the open literature? What is missing (i.e., research gaps)? What needs to be done, why and how? Clear statements of the novelty of the work should also appear briefly in the Abstract and Conclusions sections.
Changes to the manuscript: The motivation for the paper was added to the introduction, as well as the novelty added to the abstract and conclusion

Question 3: An updated and complete literature review should be conducted and should appear as part of the Introduction, while bearing in mind the work's relevance to SAE and taking into account the scope and readership of the session. The results and findings should be compared to and discussed in the context of earlier work in the literature.
Changes to the manuscript: Further literature was studied and added to the introduction

Question 4: The description of each symbol (e.g., after each equation) may be avoided if a Nomenclature is provided, otherwise, all symbols should be clearly defined at the first instance of appearance in the manuscript.
Changes to the manuscript: Abbreviations were added in page 9 and the symbols were described

Reviewer #317963

Comment 1: The values in table 2 do not add to 100% and need to be defined better
Changes to the manuscript: A description of the volumetric percentages was added to page 2 to explain that each component can inherit up to the value displayed in the table, according to the manufacturer.

Question 1: The term ignition delay needs to be better defined. The "start of combustion" can be determined several ways please elaborate on the approach and determination (apparent het release, visually observed, etc?) what was the threshold used, and was ti robust to if different terminology/definitions are used?
Discussion: This was also mentioned by Reviewer #317968, thank you both for this.
Changes to the manuscript: A description of the calculation for the ignition delay (elapsed time between first Diesel injection and first observed flames) was added to page 7 and the threshold value to page 4

Question 2: Because AHRR is being analyzed an explanation (in detail) on how this was calculated is needed. Specifically, is a shifting gamma used? How do you account for the larger crevice flows in a optical engine? Hydrogen has a very high gamma and negative molar product yield so this affects the determination of AHRR. How do such considerations change the calculations in your study? Many of the images show AHRR being positive starting at -20 CAD, this is over 5 CAD before the earliest diesel injection event. Moreover, the spray cooling of the pilot is not observed at all. Based on this (and the lack of data before -20 CAD and the lack of negative AHRR in the y-axis, this reviewer sees issues that need to be correct in the analysis.
Discussion: The negative Y-axis has been added to the graphs and the X-axis has been extended to 50 CA BTDC. The small rises of the HRR above 0 before the first injection are due to vibrations in the pressure signal. The HRR calculation was added. It uses a fixed gamma since only the in-cylinder pressure data with Crank angles was available for the calculations. The crevice flows of the engine are comparable to non-optical engines, since the tests were only run for a few cycles and the engine was motored by a dyno before and after each case to ensure that the sealing of the optical components is intact. Pilot cooling was not available for my tests at this engine. The HRR calculations are only an indication to make the cases comparable, therefore an explanation was added, that a fixed gamma is not completely accurate for calculating the dual fuel cases.

Reviewer #317968

Question 1: There is way too much in the abstract. Most of that should be places somewhere else in the paper.
Discussion: Thank you for the suggestion. I shortened the abstract accordingly.

Question 2: Intro. This would be helpful to break down into more paragraphs.
Changes to the manuscript: The introduction was broken down into more paragraphs

Question 3: More details on the experimental setup for the NG injections are needed.
Changes to the manuscript: A description explaining that the NG/Hythane was port fuel injected was added to page 2.

Question 4: Similarly, more details and motivation for using hythane is need.
Changes to the manuscript: A motivation to study Hythane due to it's faster combustion speed was added to the end of the Introduction in page 2

Question 5: I think the tables would be better with more gridlines
Changes to the manuscript: Additional Gridlines were added to the tables

Question 6: Table 4. More description is needed. Its hard to tell from the table alone that 15+5 means an injection at 15 deg and 5 deg.
Changes to the manuscript: An additional description was added, explaining that the Diesel was split injected in all cases in page 3

Question 7: Pg 3. Typically main injection refers to the diesel injection. It is very confusing the way it is currently written
Changes to the manuscript: Changed the description to Main fuel injection

Question 8: Similar to comment 3. How is the NG/Hythane injected? And how is it split up?
Changes to the manuscript: A description to the engine control system was added to page 3, which made it necessary to split the main fuel injection into two since injections. The injections with duration above 5 ms were not possible due to the limitation of the injection control system was added.

Question 9: Make it more clear somewhere the number of cycles used to do the imaging
Changes to the manuscript: The legends of Figures 6 until 12 were changed to display the minimum amount of cycles overlapping

Question 10: Table 3, how are B1 and B2 different to get the different IMEP
Discussion: Case B1 and B2 only differ in their Diesel injection timing, this is displayed in Table 4

Question 11: Define how you are calculating ign delay
Discussion: This was also mentioned by Reviewer #317963, thank you both for this.
Changes to the manuscript: A description of the calculation for the ignition delay (elapsed time between first Diesel injection and first observed flames) was added to page 7